following paper in this issue.
(10) H. P. Fritz, *Chem. Ber.*, **94**, 1217 (1961).
(11) E. O. Fischer and H. Werner, *Tetrahedron Lett.*, 17 (1961).
(12) R. B. King, "Organometallic Synthesis: Volume I, Transition Metal Compounds", Academic Press, New York, N.Y., 1965.
(13) M. L. H. Green, J. A. McCleverty, L. Pratt, and G. Wilkinson, *J. Chem. Soc.*, 4854 (1961).
(14) R. L. Cooper and M. L. H. Green, *Z. Naturforsch., Teil B*, **19**, 652 (1964).

Reactivity Patterns of Chromocene, Molybdenocene, and Tungstenocene Reaction Systems. II. An Analysis in Terms of Molecular Orbital and Electron–Electron Repulsion Energies[1a]

Hans H. Brintzinger*[1b] Lawrence L. Lohr, Jr., and Kit L. Tang Wong[1c]

Contribution from the Department of Chemistry, The University of Michigan, Ann Arbor, Michigan 48104, and Fachbereich Chemie, Universität Konstanz, D 7750 Konstanz, West Germany. *Received November 5, 1974*

Abstract: Gradations in reactivity among the group 6 metallocenes have been studied theoretically by an extended Hückel molecular orbital analysis of one-electron energy changes associated with the formation of reaction products and intermediates, and by an evaluation of the associated electron–electron repulsion energies in terms of Racah repulsion parameters. The effect of ring–metal–ring bending distortions on spin-pairing energies is described, and the results are used to express enthalpies of formation of monocarbonyl complexes. A satisfactory accounting is obtained for the different stabilities observed for $(C_5H_5)_2Cr(CO)$ and $(C_5H_5)_2Mo(CO)$. The unique stability of the 20-electron species $(C_5H_5)_2W(CO)_2$ is discussed in terms of changes in ligand repulsions, but not thoroughly understood. The formation of the dihydride $(C_5H_5)_2MoH_2$ from a $(C_5H_5)_2Mo$ intermediate and an H_2 molecule is described in detail by a correlation diagram for various electronic states; it is concluded that the activation energy for this insertion reaction is nearly equal to the spin-pairing energy associated with its transition state. Finally, the formation of tungstenocene phenyl hydride complexes by insertion into aromatic C–H bonds is discussed in terms of repulsive ligand interactions and facilitated ring dislocations similar to those held responsible for the unique stability of the tungstenocene dicarbonyl complex mentioned above.

Interesting reactivity patterns have been established for group 6 transition metal bis(cyclopentadienyl) species with a number of substrate molecules (see Table I).

Most prominent among the reactivity differences observed is the lack of reactivity of chromocene vis-a-vis virtually all substrates except CO[2] and, on the other hand, the unique tendency of tungstenocene to form a stable dicarbonyl complex (which exceeds an 18-electron configuration)[2] and to generate phenyl hydride derivatives by insertion into aromatic C–H bonds.[3,4] In order to extract from these observations some generally useful reactivity parameters for addition or insertion reactions of low-valent metal species, we have undertaken a theoretical analysis of those factors which might govern the feasibility of reactions such as those mentioned in Table I. We wish to present here computational evidence that the reactivity differences in the series under consideration are largely due to differences in interelectronic repulsion energies, namely, one-center repulsions between d electrons on the metal atom and two-center repulsions between different ligands, which are associated with the formation of products or intermediates in the reaction concerned.

Computational Methods

The computational approach utilized in this study consists of two mutually complementary parts: an analysis of one-electron orbital energies and eigenfunctions by the extended Hückel molecular orbital (EHMO) method, and a subsequent determination of the total energies for the ensuing possible d-electron configurations and their individual multielectron states by an expansion in terms of Racah electron repulsion parameters. The role of the extended Hückel calculations is to establish values of orbital splitting and mixing associated with varying geometries. The subsequent ligand field multiplet calculations then give the energies of possible multiplet states for the various geometries of the reaction complex considered. In this way, we hope to obtain an intuitively transparent break-down of the main origins of differences in reaction enthalpies and activation barriers in this series of coordinatively unsaturated compounds.

The EHMO method has been used with considerable success in the treatment of various transition metal complexes[6-8] as well as transition states and intermediates in a variety of chemical reactions.[9-11] It has been found to yield reliable estimates of optimal geometries with respect to angular parameters,[12] since the dependence of bond angles on both overlap between bonded atoms and repulsive interaction between nonbonded atoms is appropriately modeled by this method. The EHMO program used is based on a program originally written by Hoffmann[13] and modified by Bartell et al.[14] The basis orbitals for the metal atoms are single-parameter Slater-type atomic orbitals of the *n*p, *n*d, $(n + 1)$s, and $(n + 1)$p type. The *n*p orbitals of the metal are included to provide the necessary repulsion at small internuclear metal–ligand separation. The orbital exponents and diagonal energy matrix elements adopted for the calculations are given in Table II. These values, close to those employed in earlier calculations,[6,15-17] were chosen so as to yield acceptable results on the following counts: (1) ionization potentials for both metal complexes and substrate molecules close to those experimentally determined; (2) energy gaps between occupied and empty orbitals compatible with experimentally established or supported orbital occupation

Table I. Reactions of Group 6 Transition Metal Bis(cyclopentadienyl) Species $(R_5)_2M$ ($R_5 = (\eta\text{-}C_5H_5)$; M = Cr, Mo, W) with a Number of Substrate Molecules[a]

	+ CO → $(R_5)_2M\text{-}CO$	+ H_2 → $(R_5)_2MH_2$	+ C_2H_4 → $(R_5)_2M(CH_2)_2$	+ 2 CO → $(R_5)_2M(CO)_2$	+ C_2H_2 → $R_5M(H)C_2H_3$	+ C_6H_{12} → $R_5M(H)C_6H_{11}$
$(R_5)_2Cr$	±	−	−	−	−	−
$(R_5)_2Mo$	+	+	+	±	−	−
$(R_5)_2W$	+	+	+	+	+	−

[a] Symbols: +, reaction indicated proceeds under appropriate conditions, product stable under standard conditions of temperature and pressure; −, reaction does not proceed under conditions investigated, product unknown; ±, reaction incomplete, product observable but unstable at standard temperature and pressure. "$(R_5)_2Mo$" and "$(R_5)_2W$" occur as reaction intermediates only.[2-5]

Table II. Atomic Orbital Parameters

Molecule	Atom	Orbital	Slater orbital exponent	H_{ii}
	Mo	4p	4.00	−50.00
	(or W)	4d	2.50	−7.00
		5s	1.50	−5.00
		5p	1.50	−4.00
	Cr	3p	3.00	−50.00
		3d	2.20	−7.00
		4s	1.50	−5.00
		4p	1.50	−4.00
Pseudo-H_5-ring	"H"	1s	1.20	−10.00
CO	C	2s	1.40	−25.00
		2p	1.40	−11.00
	O	2s	1.60	−28.00
		2p	1.60	−14.00
C_6H_6, C_6H_5−	C	2s	1.80	−20.00
		2p	1.70	−9.00
	H	1s	1.20	−12.00
H_2	H	1s	1.20	−12.50
		2p	1.20	−2.50

patterns; (3) atomic charges in the vicinity of +1 for the metal atom and of near-zero for other atoms in both reactants and products of each reaction. The main conclusions derived from our computations are fairly independent of the specific choice of these input parameters; where such a dependence was noted, reference is made to it in the results section. No attempts were made to iterate computations with charge-dependent matrix elements so as to obtain self-consistency of charge distributions, nor did we explicitly differentiate in our calculations between molybdenum and tungsten complexes; rather, specific properties of the W derivatives were projected from the results of the corresponding Mo systems in a manner to be described later on. Off-diagonal matrix elements, H_{ij}, are evaluated by the program used according to the Wolfsberg-Helmholz equation

$$H_{ij} = 0.5K(H_{ii} + H_{jj})S_{ij}$$

where S_{ij} are the appropriate overlap integrals and K is set equal to 1.75 for all calculations.

To save calculation time, fictitious H_5 rings were used throughout these calculations to represent the π-system of each (C_5H_5) ring as "seen" by the metal. The spacing between π-levels was adjusted to values similar to those obtained in earlier, more complete calculations[6,7] by appropriate choice of orbital energies and exponents for these pseudo-ring atoms while keeping their distances within each ring equal to 1.40 Å, the value found for C-C distances in typical (C_5H_5) rings. Metal-ring distances were not varied with the objective of obtaining minimum energies for metal-to-ring bonding; rather, metal-ring distances were set so as to obtain plausible d-orbital splittings on the metal. Metal-pseudo-ring distances of 1.20 Å for $(R_5)_2Cr$ and 1.40 Å for $(R_5)_2Mo$ and $(R_5)_2W$ gave d-orbital splittings of acceptable magnitudes; these values, which represent distances between the respective metal atom and the center of the inner π-lobe on each ring, appear reasonable when compared to actual metal-ring distances of 1.66 Å for $(C_5H_5)_2Fe$ and 1.85 Å for $(C_5H_5)_2Ru$ and $(C_5H_5)_2Os$.[18-20] The geometry of the two H_5 rings is assumed to be in an eclipsed form for all systems, so that a C_{2v} symmetry results for the bent sandwich structures. For unbent structures, the resulting symmetry is D_{5h}; in keeping with general use, however, orbital designations with parity symbols g and u are given as they arise from an effective symmetry of D_{5d} or $D_{\infty h}$. Detailed geometries for intermediates and products are given in the respective results section.

Table III. Estimated Energy Parameters[a] for nd^4 Ions

Ion	B	C	ζd
Cr(II)	710	2790	220
Mo(II)	440	1990	670
W(II)	360	2100	2560

[a] All parameters in cm^{-1}; no A values are needed.

In order to assess interelectronic repulsion energies for reaction products and intermediates and their dependence on the metal involved, one could follow a full ligand field approach such as that recently reported for d^4 as well as other metallocenes by Warren.[21] We use a somewhat more restricted treatment here, in that only those terms are considered which arise from an accommodation of all four electrons in the $\delta_g(e_{2g})$ and/or $\sigma_g(a_{1g})$ set of orbitals, while terms involving one or more electrons in the $\pi_g(e_{1g})$ orbitals are not taken into account. Terms with two electrons in π_g could have configuration interaction (CI) with the terms under consideration, but this CI was considered sufficiently small to be neglected here. Electron-electron repulsion energies are then expressed in terms of Racah electron repulsion parameters, obtained from tabulated integrals valid for orbitals that are assumed to be purely metal ion nd in character.[22] While this assumption is reasonable for axially symmetric metallocenes and still acceptable for bent metallocene structures, some "nephelauxetic" reduction of repulsion parameters has to be taken into account for some of the products, where extensive interaction between metal d orbitals and ligand orbitals occurs. Estimates for Racah parameters B and C, and for spin-orbit coupling constants, ζ, for chromium, molybdenum, and tungsten are listed in Table III. Values for chromium and molybdenum are actually those obtained[23] from the atomic spectra of Cr(I) and Mo(I), thus incorporating some orbital expansion effect. Analogous values for W(I) are not available; the values for tungsten given in Table III are based on experimental values for W(0) and on the difference between experimental values for Mo(0) and Mo(I).[23]

Results and Discussion

1. Unsubstituted Metallocenes. For undistorted, axially symmetric $(R_5)_2M$ structures our EHMO calculations yield the following orbital level ordering: $\delta_g(e_{2g}$; predominantly $d_{x^2-y^2}$, d_{xy}; slightly bonding with $R_5\pi$ orbitals) < $\sigma_g(a_{1g}$;

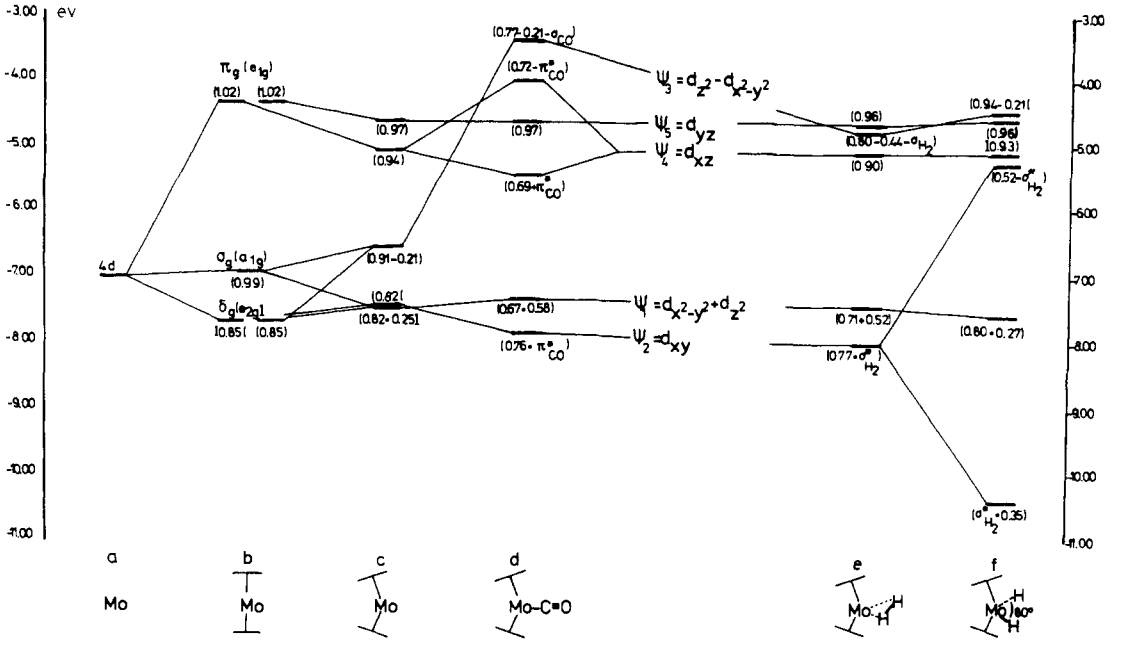

Figure 1. Energies (in eV) and d orbital coefficients for highest occupied and lowest empty molecular orbitals of various molybdenocene derivatives: (a) assumed d-orbital energy of Mo center, (b) $(C_5H_5)_2Mo$, axial symmetry ($\omega = 0°$), (c) $(C_5H_5)_2Mo$, bent structure with $\omega = 40°$, (d) $(C_5H_5)_2Mo(CO)$, with $\omega = 40°$ and $r_{M-CO} = 2.05$ Å, (e) transition state for insertion into H_2 (cf. Figure 6), (f) $(C_5H_5)_2MoH_2$, with $\omega = 40°$ and $r_{Mo-H} = 1.60$ Å.

Table IV. Term Energies[a] for nd^4 Metallocenes

Configuration	Term	*a*	*b*	*c*	*d*	*s*
δ_g^4	$^1\Sigma_g^+ + b$	6	24	8	4	0
$\delta_g^3\sigma_g^1$	$^1\Delta_g$	6	0	7	3	1
	$^3\Delta_g c$	6	−8	5	3	1
$\delta_g^2\sigma_g^2$	$^1\Sigma_g^+ + b$	6	−16	9	2	2
	$^1\Gamma_g$	6	−16	7	2	2
	$^3\Sigma_g^-$	6	−16	5	2	2

[a] Each energy given in the form $E = aA + bB + cC + d\lambda_\delta + s\lambda_\sigma$, where *A*, *B*, and *C* are Racah parameters and λ_δ and λ_σ are orbital energies. [b] Electron repulsion matrix element of $\sqrt{2}(4B + C)$ connects the two $^1\Sigma_g^+$ terms. [c] First-order spin–orbit splitting with energies $+\zeta_d$, 0, and $-\zeta_d$ for levels with $\Omega = 1$, 2, and 3, respectively.

predominantly $d_{3z^2-r^2}$; virtually nonbonding) < $\pi_g(e_{1g}$; predominantly d_{xz}, d_{yz}; antibonding with $R_5\pi$ orbitals). The energy gaps $\Delta E(\pi-\sigma)$ and $\Delta E(\sigma-\delta)$ are determined by the interaction between metal d orbitals and ligand π orbitals; from our choice of input parameters we obtain $\Delta E(\pi-\sigma)$ = 23,200 cm^{-1} and $\Delta E(\sigma-\delta)$ = 7200 cm^{-1} for $(R_5)_2Cr$ and $\Delta E(\pi-\sigma)$ = 20,000 cm^{-1} and $\Delta E(\sigma-\delta)$ = 6000 cm^{-1} for $(R_5)_2Mo$ (Figure 1). Electron configurations of interest for such an orbital pattern are δ_g^4, $\delta_g^3\sigma_g^1$, and $\delta_g^2\sigma_g^2$ which give rise to a total of six electronic states.[24] The energy for each of these states is given in Table IV, in the form $E = aA + bB + cC + d\lambda_\delta + s\lambda_\sigma$ where λ_δ and λ_σ are orbital energies and *A*, *B*, and *C* are Racah parameters. A configuration interaction matrix element of magnitude $\sqrt{2}(4B + C)$ connects the two $^1\Sigma_g^+$ terms arising from δ_g^4 and $\delta_g^2\sigma_g^2$, respectively. In addition, we note that a first-order spin-orbit splitting occurs for the $^3\Delta_g$ state, with energies of $+\zeta$, 0, and $-\zeta$ for levels with $\Omega = 1$, 2, and 3, respectively.

The energies for each of these states are plotted in Figures 2 and 3 for chromium and molybdenum, as a function of the orbital energy difference $\Delta E(\sigma-\delta)$, with the energy of the $^3\Delta_g$ and $^1\Delta_g$ terms from $\delta_g^3\sigma_g^1$ taken to remain constant. Thus the energies of all the terms from $\delta_g^2\sigma_g^2$ have unit positive slope, while the term from δ_g^4 has unit negative slope. However, a strong CI between the two $^1\Sigma_g^+$ terms

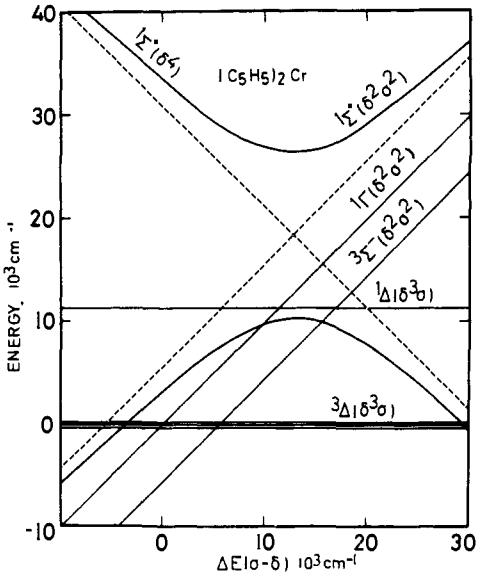

Figure 2. Term energies as a function of the difference in $\sigma_g(m_l = 0)$ and $\delta_g(m_l = \pm 2)$ orbital energies for the δ_g^4, $\delta_g^3\sigma_g^1$, and $\delta_g^2\sigma_g^2$ configurations of chromocene assuming $D_{\infty h}$ symmetry, energy expressions from Table IV and parameters from Table III. For the two $^1\Sigma_g^+$ terms, the dashed straight lines indicate energies without configuration interaction (CI), while the two branches of the solid curved lines indicate energies with CI; the lower branch of the $^1\Sigma^+$ state (not labeled in figure) changes from a predominant $\delta^2\sigma^2$ configuration (at left) to predominantly δ^4 (at right).[24]

modifies this result, as the curved lines in Figures 2 and 3 show. We observe for chromocene that the ground state is $^3\Sigma_g^-$ term, with an electron repulsion energy lower by 8*B* than that for $^3\Delta_g$, lies only a few thousand wave numbers above $^3\Delta_g$ in this region of $\Delta E(\sigma-\delta)$. We also note that trends were discussed by Warren[21] using somewhat different parameters. The $^3\Delta_g$ term corresponds to the $^3E_{2g}$ term in D_{5d} symmetry that Rettig and Drago[7] have indicated as most likely being the ground term. Our EHMO results of

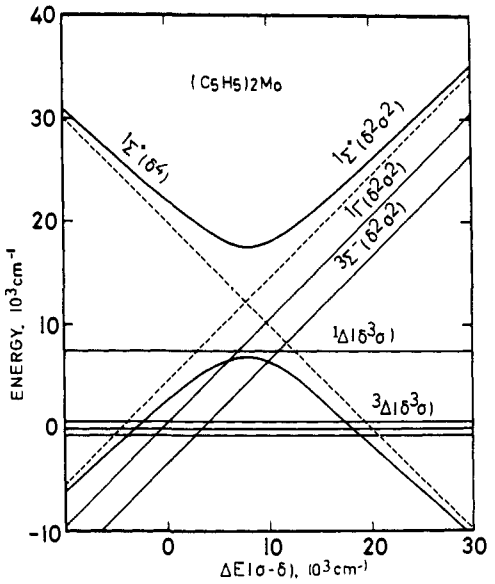

Figure 3. Term energies as in Figure 2, but for molybdenocene.

$\Delta E(\sigma-\delta)$ = 7200 cm^{-1} for chromocene are in accord with this assignment and would imply the triplet term $^3\Delta_g$ as the ground state for chromocene. We note, however, that the $^3\Sigma_g^-$ term, with an electron repulsion energy lower by $8B$ than that for $^3\Delta_g$, lies only a few thousand wave numbers above $^3\Delta_g$ in this region of $\Delta E(\sigma-\delta)$. We also note that there are three singlet terms with energies approximately 10,000 cm^{-1} above $^3\Delta_g$. These are $^1\Sigma_g^+$, $^1\Gamma_g$, and $^1\Delta_g$. The other $^1\Sigma_g^+$ is at an energy of 26,800 cm^{-1}. The highly unfavorable energy of this state arises from the requirement for a δ_g^4 configuration to place all four of the metal valence electrons into orbitals in the equatorial plane of the sandwich molecule. Those states, on the other hand, which are based on a configuration with two electrons each in the equatorial δ_g and the axial σ_g orbitals lead to a substantially reduced electron repulsion.

The molybdenocene results in Figure 3 are similar to those for chromocene, except that the range of stability for the $^3\Delta_g$ term is only for orbital splittings from 3500 to 18,000 cm^{-1}, and that all triplet-singlet separations are reduced because of the smaller Racah parameters for molybdenum as compared to those for chromium. Nevertheless, our EHMO results of $\Delta E(\sigma-\delta)$ = 6000 cm^{-1} indicate that the triplet term $^3\Delta_g$ is almost certainly the ground state for an $(R_5)_2Mo$ reaction intermediate with an assumed axially symmetric structure. Accordingly, this state will be considered henceforth as the reference state for our further studies of reaction and activation enthalpies involving the species $(R_5)_2Mo$. The tungstenocene results closely resemble those shown for molybdenocene in Figure 3 because similar Racah parameters were chosen (Table III). However, the large ζ value for tungsten results in a large spin-orbit splitting of the $^3\Delta_g$ term, with an Ω = 3 ($M_j = \pm 3$) level stabilized by an additional 2500 cm^{-1}. Therefore, the three lowest singlet states, $^1\Delta_g$, $^1\Gamma_g$, and $^1\Sigma_g^+$ are found again about 10,000 cm^{-1} above the lowest $^3\Delta_g$ state for tungstenocene for orbital splittings of $\Delta E(\sigma-\delta)$ = 6-8000 cm^{-1}.

As an approach to the formation of reaction intermediates and products, we now consider the bending of the ring-metal-ring bond angle, thus reducing the assumed axial symmetry to the C_{2v} symmetry of a bent eclipsed sandwich molecule the geometry of which is given in Figure 4. This distortion removes all orbital degeneracies, and we obtain

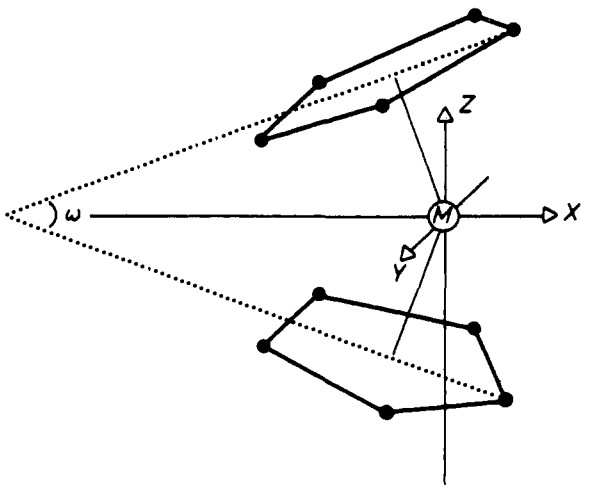

Figure 4. Assumed geometry for bent metallocenes.

an energy diagram such as the one given for an angle ω = 40° in Figure 1 for the orbitals with predominant d character. We note that the atomic orbitals $d_{3z^2-r^2}$ and $d_{x^2-y^2}$ get mutually admixed in orbitals Ψ_1 and Ψ_3 (both of a_1 symmetry), while Ψ_2 is of b_1 symmetry and contains only d_{xy}. In order to simplify an analysis of electron repulsion energies, we approximate these molecular orbitals as follows.

$$\Psi_3 = (1+\alpha^2)^{-1/2}[d_{3z^2-r^2} - \alpha d_{x^2-y^2}] \quad (1a)$$

$$\Psi_2 = d_{xy} \quad (1b)$$

$$\Psi_1 = (1+\alpha^2)^{-1/2}[d_{x^2-y^2} + \alpha d_{3z^2-r^2}] \quad (1c)$$

This notation (eq 1) allows us to expand the four-electron wave functions for various possible electron configurations of the bent molecule in terms of the states of the original, axially symmetric structure and thus to evaluate the respective electron repulsion terms.

For the $^1A_1$ term corresponding to the electron configuration $\Psi_1^2\Psi_2^2$, for example, the four-electron wave function may be expanded in terms of the wave functions used to construct Table IV, as follows (cf. eq 1).

$$^1A_1(\Psi_1^2\Psi_2^2) = (1+\alpha^2)^{-1}\{^1\Sigma_g^+(\delta_g^4) + 2^{-1/2}\alpha^2 \times [^1\Sigma_g^+(\delta_g^2\sigma_g^2) + {}^1\Gamma_g(\delta_g^2\sigma_g^2)] + 2^{1/2}\alpha\,{}^1\Delta_g(\delta_g^3\sigma_g^1)\} \quad (2)$$

Since the only cross term in the repulsion energy is $\sqrt{2}(4B + C)$, connecting the two $^1\Sigma_g^+$ states, the associated electron repulsion energy is readily shown to be

$$E[^1A_1(\Psi_1^2\Psi_2^2)] = 6A + 8(3-2\alpha^2)B/(1+\alpha^2) + 8C \quad (3)$$

where α is some function of the deformation angle ω. For α values close to unity, the singlet state $^1A_1(\Psi_1^2\Psi_2^2)$ has a reasonably low electron repulsion energy of about $4B + 8C$, and will then represent the lowest available singlet state; for reasonable orbital splittings $^1A_1$ is the ground state of reaction products and transition states of interest. For small values of α, however, $^1A_1$ correlates with the high energy δ_g^4 configuration ($^1\Sigma^+$ term); here, $^1A_1(\Psi_1^2\Psi_2^2)$ is higher in energy, therefore, than other singlets derived from electron configurations with lower electron repulsion energies. Some of these correspondences for $\alpha \to 0$ are

$$\Psi_1^2\Psi_3^2 \to 2^{-1/2}\{^1\Sigma_g^+(\delta_g^2\sigma_g^2) - {}^1\Gamma_g(\delta^2\sigma^2)\} \quad (4a)$$

$$\Psi_2^2\Psi_3^2 \to 2^{-1/2}\{^1\Sigma_g^+(\delta_g^2\sigma_g^2) + {}^1\Gamma_g(\delta_g^2\sigma_g^2)\} \quad (4b)$$

$$\Psi_1^2\Psi_2\Psi_3 \to {}^{1,3}\Delta_g(\delta_g^3\sigma_g^1);\ B_1 \text{ components in } C_{2v} \quad (4c)$$

$$\Psi_2^2\Psi_1\Psi_3 \to {}^{1,3}\Delta_g(\delta_g^3\sigma_g^1);\ A_1 \text{ components in } C_{2v} \quad (4d)$$

$$\Psi_2^2\Psi_1\Psi_2 \to {}^1\Gamma_g(\delta_g^2\sigma_g^2),\ {}^3\Sigma_g(\delta_g^2\sigma_g^2) \quad (4e)$$

Table V. Transformed Electron Repulsion Integrals

No.	Integral[a]	a	b	c
1	$[\Psi_1^2, \Psi_1^2]$	1	4	3
2	$[\Psi_2^2, \Psi_2^2]$	1	4	3
3	$[\Psi_3^2, \Psi_3^2]$	1	4	3
4	$[\Psi_1^2, \Psi_2^2]$	1	$4(1-\alpha^2)/(1+\alpha^2)$	1
5	$[\Psi_1^2, \Psi_3^2]$	1	−4	1
6	$[\Psi_2^2, \Psi_3^2]$	1	$-4(1-\alpha^2)/(1+\alpha^2)$	1
7	$[\Psi_1\Psi_2, \Psi_2\Psi_1]$	0	$4\alpha^2/(1+\alpha^2)$	1
8	$[\Psi_1\Psi_3, \Psi_3\Psi_1]$	0	4	1
9	$[\Psi_2\Psi_3, \Psi_3\Psi_2]$	0	$4/(1+\alpha^2)$	1

[a] Each integral is evaluated with respect to the wave functions given in eq 1 and is listed in terms of the coefficients *a*, *b*, and *c* of the Racah parameters *A*, *B*, and *C*, respectively. The symbol $[\Psi_a\Psi_b, \Psi_c\Psi_d]$ denotes the repulsion integral $\int\int\Psi_a^*(1)\Psi_b(1)(e^2/r_{12})\Psi_c^*(2)\Psi_d(2)\,d\tau_1\,d\tau_2$. Additional integrals needed for configuration interaction calculations are $[\Psi_1\Psi_3, \Psi_2^2] = [\Psi_1\Psi_2, \Psi_2\Psi_3] = -8\alpha B/(1+\alpha^2)$ and $[\Psi_1\Psi_3, \Psi_1^2] = [\Psi_1\Psi_3, \Psi_3^2] = 0$.

For finite values of the mixing coefficient α, the electron repulsion energies are best evaluated from the transformed electron repulsion integrals listed in Table V. For the lowest triplet $^3B_1$, associated with the configuration $\Psi_1^2\Psi_2\Psi_3$, one obtains an electron repulsion energy of

$$E[^3B_1(\Psi_1^2\Psi_2\Psi_3)] = 6A - 8(1+2\alpha^2)B/(1+\alpha^2) + 5C \quad (5)$$

The triplet-singlet separation is therefore obtained as

$$\Delta E[^1A_1(\Psi_1^2\Psi_2^2) - {}^3B_1(\Psi_1^2\Psi_2\Psi_3)] = 32B/(1+\alpha^2) + 3C - (\lambda_3 - \lambda_2) \quad (6)$$

where λ_2 and λ_3 are orbital energies appropriate to Ψ_2 and Ψ_3. We note that the triplet-singlet separation for the axially symmetric structure

$$\Delta E[^1\Sigma_g^+(\delta_g^4) - {}^3\Delta_g(\delta_g^3\sigma_g^1)] = 32B + 3C - (\lambda_\sigma - \lambda_\delta) \quad (7)$$

has been reduced by the factor $(1+\alpha^2)^{-1}$ in the coefficient of *B* for the bent metallocene. We conclude that one effect of bending is to reduce the spin-pairing energy by mixing the $d_{x^2-y^2}$ orbital partially with $d_{3z^2-r^2}$ (eq 1); this effect resembles the CI effect previously discussed, in that greater avoidance of the electrons is achieved by placing part of the electron population out of the equatorial plane, into the $d_{3z^2-r^2}$ orbital.

Other triplets are $^3A_1(\Psi_2^2\Psi_1\Psi_3)$ derived from $^3\Delta_g(\delta_g^3\sigma_g^1)$ and $^3B_1(\Psi_3^2\Psi_1\Psi_2)$ from $^3\Sigma_g^-(\delta_g^2\sigma_g^2)$. Of these, the triplet state $^3B_1(\Psi_1^2\Psi_2\Psi_3)$, derived from $^3\Delta_g(\delta_g^3\sigma_g^1)$ in axial symmetry, will remain the ground state throughout the extent of the bending coordinate studied. The triplet state $^3A_1(\Psi_2^2\Psi_1\Psi_3)$, however, which is also derived from $^3\Delta_g(\delta_g^3\sigma_g^1)$ (and has an electron repulsion energy of $6A - 8B + 5C$ for all values of α), is almost indistinguishable in energy from $^3B_1(\Psi_2^2\Psi_1\Psi_3)$, and will become more stable than the latter whenever a ligand approaches the metal along the *x* axis (see discussion below).

For a d^4 metallocene in such an electron configuration, our EHMO results indicate a near-parabolic potential surface for the ring-metal-ring bending mode, with a force constant somewhat greater for chromocene than for molybdenocene. An energy of 6300 cm^{-1} is required to tilt the rings to an angle of $\omega = 40°$ for $(R_5)_2Cr$ as compared to 5350 cm^{-1} for $(R_5)_2Mo$.

2. Monocarbonyl Complexes. The three group 6 monocarbonyl complexes, $(R_5)_2M(CO)$, are known to be diamagnetic.[2] Our results indicate that, in the formation of these complexes, significant repulsion among the metal d electrons has to be overcome. Based on the input parameters listed in Table II, orbital splitting patterns such as that given in Figure 1 are obtained for $(R_5)_2M(CO)$. For the ground state configuration $\Psi_1^2\Psi_2^2$, one obtains a near-parabolic dependence of total energies on the angle ω, with an energy minimum at $\omega = 40°$; this value is certainly plausible when compared with those obtained experimentally for related $(R_5)_2M$ derivatives.[25] The one-electron energy change associated with the formation of molybdenocene monocarbonyl in its $^1A_1$ state from normal $^3\Delta_1$ molybdenocene and carbon monoxide is calculated by EHMO as $\Delta E = -21{,}000$ cm^{-1}. About half of this energy change must be absorbed, however, by the d-electron repulsion associated with the multiplicity change in going from the paramagnetic reactants to the diamagnetic product. For a mixing coefficient $\alpha = 0.87$ present in this carbonyl complex, eq 3 yields an electron repulsion energy of about 18,500 cm^{-1} for $(R_5)_2Mo(CO)$ in $^1A_1$, about 12,000 cm^{-1} in excess of that calculated for the initial $^3\Delta_g$ state of $(R_5)_2Mo$ (6,400 cm^{-1}). Hence, a net enthalpy of complex formation of scarcely more than −9000 cm^{-1} or about −26 kcal/mol is expected from our theoretical analysis, a reasonable, albeit probably somewhat low estimate. We can now immediately appreciate the main origin of the reduced stability of the chromocene monocarbonyl. Here, a substantially higher spin pairing energy of close to 20,000 cm^{-1} works against the formation of the singlet state of this complex. In addition, our EHMO results indicate that repulsive interactions between the orbitals of the carbonyl ligand and those of the more closely situated R_5-rings further reduce the one-electron energy gain for the formation of $(R_5)_2Cr(CO)$. The experimentally observed enthalpy of complex formation of about −18 kcal/mol (about −6000 cm^{-1}) indicates that our theoretical estimates are somewhat too pessimistic here. At this point, the intrinsic limitations of our theoretical approach become obvious. Interelectronic repulsion is treated as a first-order perturbation here, yet its magnitude is found to be comparable to that of one-electron energy changes associated with complex formation. An explicit consideration of these interelectronic repulsion potentials would therefore require nontrivial adaptions of the molecular wave functions. Experimentally, such effects are indicated, e.g., by the ir shifts observed for the CO ligand in the metallocene monocarbonyl complexes; the substantially higher degree of back-donation observed for $(C_5H_5)_2Cr(CO)$ as compared to its molybdenum and tungsten homologs arises most likely as a consequence of increased repulsion among the d electrons on Cr compared to Mo or W centers. Nevertheless, the experimentally estimated difference of about 8-10,000 cm^{-1} between the complex formation enthalpies of $(R_5)_2Cr(CO)$ and $(R_5)_2Mo(CO)$[2] is explained surprisingly well by our simple analysis of the respective spin-pairing energies.

Concerning the dynamics of carbonyl complex formation, we have carried out an analysis of the complex formation reaction coordinate with CO approaching $(R_5)_2Mo$ along the *x* axis toward its equilibrium position, while the angle between the two (R_5) rings is steadily increased. The results (Figure 5) indicate that any activation barrier present must be comparatively small (about 2000 cm^{-1}). The initial triplet ground state $^3A_1$ does not become appreciably repulsive along this reaction coordinate until the M-C distance is decreased to well below 2.5 Å, where the singlet state is already strongly binding with respect to the reactants, so that a smooth cross-over from the initial triplet to the final singlet state occurs at an M-C distance of about 2.7 Å. This absence of any noticeable activation barrier manifests itself in the observed rate of the reaction $(R_5)_2Cr + CO \rightarrow (R_5)_2Cr(CO)$ which proceeds virtually instantaneously even at −78° in petroleum ether solution, and in the efficiency of CO as a trapping reagent for free molybdenocene and tung-

stenocene species arising as intermediates in a number of reaction systems.[2,5]

For the photolysis of the carbonyl complex $(R_5)_2Mo(CO)$ to $(R_5)_2Mo + CO$, we would predict a high quantum yield. The lowest excited singlet state of $(R_5)_2Mo(CO)$, $^1A_2(\Psi_2^2\Psi_1\Psi_4)$, must be placed about 16,000 cm^{-1} above the ground state from spectral observations; from Figure 5 it is obvious that this excited state will lead directly to the photoproducts CO and $(R_5)_2Mo$ in its triplet ground state and that the singlet state $^1A_1$ of a molybdenocene intermediate is not likely to arise as a product when $(R_5)_2Mo(CO)$ is photolyzed.

3. Dicarbonyl Complexes. Obviously, the unique stability of the tungstenocene dicarbonyl complex $(R_5)_2W(CO)_2$ vis-a-vis both its chromocene and molybdenocene analogs cannot be explained by a similar analysis of electron-repulsion terms. Differences in these terms between molybdenum and tungsten are quite undramatic; in addition, both reactants and products of a reaction, $(R_5)_2M(CO) + CO \rightarrow (R_5)_2M(CO)_2$, are diamagnetic and cannot entail any significant changes in spin pairing energies. EHMO calculations clearly indicate, on the other hand, that repulsive interactions between the CO ligands and the R_5 ring ligands are determining the stability of these dicarbonyl complexes.

One-electron energies indicate for the dicarbonyl complex $(R_5)_2Mo(CO)_2$ an instability with respect to $(R_5)_2Mo(CO) + CO$ for any prima facie dicarbonyl structure, i.e., for M-C bond lengths around 2.0 Å and C-M-C angles between 80 and 120°. This instability of the dicarbonyl complex arises from a sizeable repulsive overlap between π orbitals of the laterally placed CO ligands and those of the two ring ligands. Accordingly, one finds an anomalous increase in stability if the two ring ligands are displaced parallel to the x axis, while an optimal metal carbonyl geometry is retained. For an equilibrium OC-M-CO bond angle of 90° and a displacement of the two rings by 1 Å in the negative x direction, one calculates a one-electron energy change totaling to $-19{,}000$ cm^{-1} with respect to $(R_5)_2Mo(CO)$ in its equilibrium configuration and free CO. We have not searched further for any energy minima arising from an unsymmetrical displacement of the ring ligands, such as that mentioned in ref 2. Irrespective of the detailed equilibrium geometry for such a dicarbonyl complex, it appears certain that a substantial displacement of the ring ligands from their position normal to the metal-ring center bond has to occur in order to stabilize this complex with respect to loss of one of the CO ligands. Although our crude calculations do not present a distinct differentiation between the molybdenum and tungsten systems they do provide a qualitative clue for explaining the observed differences between these group 6 metallocene systems. For the tungsten system, the two cyclopentadienyl rings appear to be more easily dislocated so that a stable dicarbonyl complex can be formed. In contrast, the force constants for dislocations of the two rings must be substantially larger for the chromium and molybdenum systems. While we cannot further analyze the cause of this difference in dislocation force constants among the group 6 metal sandwiches at present, its effects appear to manifest themselves in other observables as well (see section 5 below).

4. Dihydrides and Related Derivatives. Since compounds of the type $(R_5)_2MH_2$ are fairly well-investigated experimentally, we have used a theoretical analysis of their properties as a point of reference for the method utilized. Green et al.[26] have collected structural data on a series of $(\eta\text{-}C_5H_5)_2MX_2$ transition metal complexes and found that the X-M-X bond angle decreases as the number of "nonbonding" d electrons increases. These authors further conclude that the lone pair of electrons in $(\eta\text{-}C_5H_5)_2MoH_2$ are located in the laterally expanding orbital Ψ_1, as suggested by Alcock,[27] rather than in the orbital Ψ_3 which is primarily extending along the x axis. The results from our calculations on $(R_5)_2MoH_2$ support this assignment (see Figure 1), in that we find Ψ_1 to be the highest filled molecular orbital. In addition, our calculations yield a fairly small equilibrium H-M-H angle of 80°, in close agreement with X-M-X angles reported by Green et al.[26] for isoelectronic $(R_5)_2MX_2$ complexes.

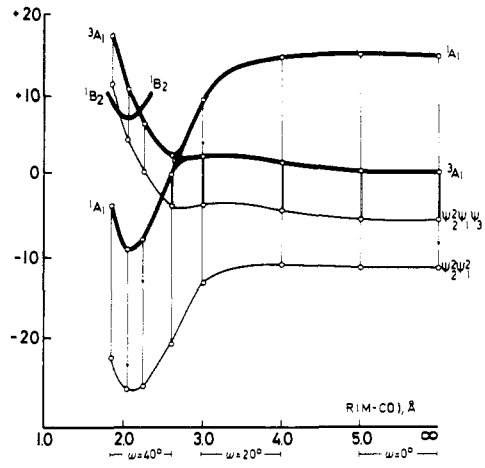

Figure 5. Correlation diagram for the approach of a CO ligand molecule along the x axis of $(C_5H_5)_2Mo$: thin lines, one-electron energies calculated by EHMO for electron configurations $\Psi_2^2\Psi_1^2$, and $\Psi_2^2\Psi_1\Psi_3$; heavy lines, energies for triplet state $^3A_1(\Psi_2^2\Psi_1\Psi_3)$ and singlet state $^1A_1(\Psi_2^2\Psi_1^2)$; vertical lines, electron repulsion energies calculated from Table V. (Energies given in 10^3 cm^{-1}; energy of excited singlet $^1B_2$ estimated from spectral data; angle ω between R_5 rings optimized in steps of 20° for each M-CO distance.)

For the enthalpy of formation of the dihydride from H_2 and $(R_5)_2Mo$ in its normal $^3\Delta_g$ state, we calculate by the EHMO method a one-electron energy change of $-14{,}500$ cm^{-1}. As for an estimate of the spin pairing contribution to the enthalpy of formation of this diamagnetic product, our method of analysis cannot be applied in a straightforward fashion. Firstly, the virtually nonbonding character of $d_{x^2-y^2}$ with respect to the two H ligands, as opposed to their significant overlap with $d_{3z^2-r^2}$, reduces the mutual admixture of these two d orbitals to the point where Ψ_1 contains almost only $d_{x^2-y^2}$ and α would be too small to justify the assumptions inherent in eq 6. In addition, the preponderant electron configuration of $(R_5)_2MoH_2$ can no longer be considered to be d^4; rather, a substantially complete transfer of electrons from Ψ_2 into the σ^* type combination of hydrogen 1s orbitals leads to a preponderant d^2 configuration, for which a significantly reduced electron repulsion is to be expected. Of these two counteracting effects, the latter is the potentially more powerful; therefore we would expect the electron repulsion energy for $(R_5)_2MoH_2$ to be smaller than that of, e.g., $(R_5)_2Mo(CO)$. A somewhat more detailed estimate of these relationships can be gleaned from an analysis of the reaction coordinate for the reaction $(R_5)_2Mo + H_2 \rightarrow (R_5)_2MoH_2$, which we wish to discuss here in some detail to exemplify our approach to the evaluation of activation energies for insertion reactions in general (Figure 6).

When a hydrogen molecule is made to approach a $(R_5)_2Mo$ metallocene species, its σ and σ^* orbitals will interact increasingly with d (and other) orbitals on the metal. Transfer of electron density from metal Ψ_2 into σ^* and from σ into metal Ψ_3 will lead to a continuous weakening of the H-H bond until, at some distance from the metal center, the two H atoms can be separated without further ex-

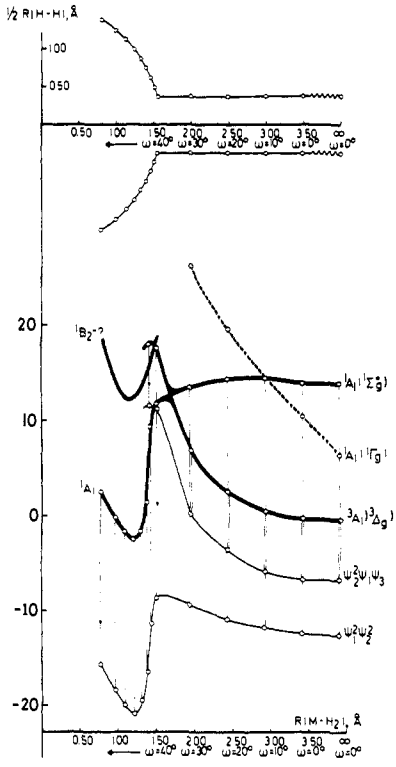

Figure 6. Formation of $(C_5H_5)_2MoH_2$ by approach of an H_2 molecule along the x axis of $(C_5H_5)_2Mo$: top, reaction coordinate studied (see text); bottom, correlation diagram for triplet state $^3A_1(\Psi_2^2\Psi_1\Psi_3)$ and singlet state $^1A_1(\Psi_2^2\Psi_1^2)$; angle ω between R_5 rings optimized in steps of 10° for each M-H_2 distance; other details as in Figure 5.

penditure of energy; they will then slide into their final positions in the product with an energy release corresponding to the H-Mo-H deformation potential. In reality, the equilibrium H-H distance will probably increase continuously with decreasing distance from the metal center; however, a somewhat artificial albeit convenient simplification of the reaction coordinate arises from a peculiar failing of the EHMO method. The experimentally established H-H distance of 0.74 Å does not correspond to an energy minimum in these calculations, as no repulsive interactions are built in here to balance the mutual approach of the hydrogen atoms in H_2. Hence, the H_2 molecule is kept at a fixed H-H bond length of 0.74 Å by an attractive potential until, at a given distance from the metal, the force constant along the H-H bond becomes negative, due to the interaction with the metal. This opening up of the H-H bond is found to occur at a position just 1.50 Å from the metal, i.e., at an Mo-H distance very close to 1.60 Å, the assumed equilibrium Mo-H distance in the product. The H atoms can be assumed then to move directly along a circular segment of radius 1.60 Å toward their equilibrium positions. The "opening point" at the intersection between the parallel and the circular sections of this reaction coordinate is its state of highest energy and is therefore considered the transition state for the reaction in question. Energies of activation calculated in this fashion are undoubtedly higher than those for a properly equilibrated H_2 molecule with a continuously adapted H-H bond length. The somewhat nonoptimal cross-section through the energy hyperface resulting from this shortcoming of the EHMO method, which requires us to place an intact H_2 molecule in direct bonding interaction with the metal, allows for an intuitively appealing inspection of the main barriers to insertion reactions of this type, however. The orbital splittings calculated for the transition state just described are presented in Figure 1. It is immediately apparent that both energies and eigenfunctions for Ψ_1, Ψ_2, and Ψ_3 are quite similar for this intermediate $(R_5)_2Mo(H_2)$ to those for the corresponding monocarbonyl complex $(R_5)_2Mo(CO)$. This similarity undoubtedly results from the equivalence between a π^* orbital in CO and a σ^* orbital in H_2, and between a σ lone pair in CO and a σ bonding pair in H_2, with respect to their interactions with metal d orbitals of symmetry b_1 and a_1, respectively.[28] An immediate consequence of this result is the requirement that the transition state in question be diamagnetic. A correlation diagram for the relevant terms $^3A_1(\Psi_2^2\Psi_1\Psi_3)$, with electron repulsion energy equal to that of $^3\Delta_g$, and $^1A_1(\Psi_1^2\Psi_2^2)$, with electron repulsion energy as given by eq 3, is given in Figure 6 together with the one-electron energies calculated by EHMO.[30] The one-electron energy for $\Psi_2^2\Psi_1\Psi_3$ is found to be quite repulsive, while that for $\Psi_1^2\Psi_2^2$ is only slightly repulsive for the approach to the transition state. By chance, this energy for $\Psi_1^2\Psi_2^2$ at the transition state (TS) almost coincides with that for $\Psi_2^2\Psi_1\Psi_3$ at infinite distance. As a consequence—and we consider this as one of the most important aspects of our analysis—*the activation energy for the insertion reaction* $(R_5)_2Mo + H_2 \rightarrow (R_5)_2MoH_2$ *is practically equal to the spin-pairing energy associated with its transition state.* Because of the near-coincidence of the corresponding one-electron energies, the energy difference between $^3A_1$ at infinite distance and $^1A_1$ at TS is just about equal to the difference between the electron repulsion energies for these two terms. More accurately, we estimate an activation energy of about 13,000 cm^{-1} or about 35 kcal/mol for this insertion reaction. The triplet and singlet terms cross along the reaction coordinate at a position about 1.8 Å from the metal. We can expect a smooth transition of the reaction system along the lower branch, since the large spin-orbit coupling constants for 4d and 5d metals provide for a finite interaction between the two terms at their intersection region.

As for the approach from the transition state to the final product, it is difficult to estimate electron repulsion energies for reasons discussed above. The observation that the dihydride is photolyzed to $(R_5)_2Mo$ and H_2[3] can be used, however, to place the final product, at least approximately, in Figure 6. Obviously, its energy cannot be lower than that of the transition state by much more than the photon energy. Uncertainties arise as to the detailed photon energy requirements or to the exact position of the excited state involved. In Figure 6 we have placed the final product by 15,000 cm^{-1} below the transition state, an estimate which we consider accurate to within ±5000 cm^{-1}. This estimate would in fact imply an electron repulsion energy in $(R_5)_2MoH_2$ smaller than that in the transition state, in accord with our discussion above. It would further predict that the overall reaction $(R_5)_2Mo + H_2 \rightarrow (R_5)_2MoH_2$ is only slightly exothermic. For the enthalpy of the related reaction $(C_5(CH_3)_5)_2Ti + H_2 \rightarrow (C_5(CH_3)_5)_2TiH_2$ we have experimentally obtained a similarly low value of about −4000 cm^{-1}.[31] The greater thermal stability of $(C_5H_5)_2MoH_2$ as compared to its groups 4 analogs, would thus appear to be exclusively of kinetic, rather than of thermodynamic nature.

For the photolysis reaction of $(R_5)_2MoH_2$ to H_2 and $(R_5)_2Mo$, one would expect a low quantum yield from Figure 1 and Figure 6. A number of excited states are predicted at energies close to that of the transition state.[32] Deactivation into these states will always compete with reaction to the photoproducts for any of the sufficiently activated states of $(R_5)_2MoH_2$, in contrast to the photolysis of $(R_5)_2Mo(CO)$, where the lowest excited state can lead directly to the formation of photoproducts without the intervention of an activation barrier.

We now want to attempt a qualitative analysis of the influence which various "chemical" parameters might have on the height of the activation barriers for insertion reactions of the type discussed above. For any d^4 metallocene, the sizeable $^3A_1 \rightarrow {}^1A_1$ spin pairing energy must immediately be reflected in the activation energy for such a reaction; this would make such a species an unlikely candidate for participation in catalytic reaction cycles depending on a facile interplay of oxidative additions and reductive eliminations. For an analogous d^3 metallocene, the spin pairing energy required to reach the corresponding $^2A_1(\Psi_2{}^2\Psi_1)$ term of the transition state from the $^4B_1(\Psi_1\Psi_2\Psi_3)$ ground state at infinite distance is further increased by about $2B + C$,[33] so that we would expect an even higher activation energy for any insertion reaction of such a d^3 metal species when compared to an analogous d^4 metallocene reaction system. For d^2 metallocenes, finally, the change in electron repulsion energy in going from the $^3B_1(\Psi_2\Psi_3)$ or $^3A_1(\Psi_1\Psi_3)$ states of the reactants at infinite distance to the $^3B_1(\Psi_1\Psi_2)$ transition state cannot amount to more than a few thousand wave numbers.[34] Based on the results presented in Figure 1 and Figure 6, we would therefore expect a d^2 metallocene species to be the kinetically most active insertion reagent in the d^n series considered.[35] The observed kinetic facility of the reaction $(C_5(CH_3)_5)_2Ti + H_2 \rightarrow (C_5(CH_3)_5)_2TiH_2$ and of its reverse[36] do attest to the validity of this projection. For any given d^n configuration, the established analogies between the complex $(R_5)_2M(CO)$ and the transition state $(R_5)_2M(H_2)$ (Figure 1) suggest that every change in the metal or its environment which tends to stabilize coordination of a CO molecule (e.g., by increased capability for back-donation) can also be expected to make the transition state for an insertion reaction more easily available.

As for insertion reactions with substrates other than H_2, the question arises of why these insertions are often so much more difficult to achieve or, in fact, virtually unknown as in the case of insertion into C–C bonds. The answer to this question cannot lie in thermodynamic relationships, since the C–C bond in an alkane such as ethane is in fact weaker than the H–H bond in H_2, and since metallocene dialkyl derivatives such as $(\eta\text{-}C_5H_5)_2Mo(CH_3)_2$ appear to be thermally at least as stable as the analogous dihydrides.[5b] We must conclude then that a particularly unfavorable activation energy precludes insertion into C–C bonds. The unavailability of the transition state of this reaction is probably best demonstrated by the fact that even the statistically favored reverse reaction—decomposition of a metallocene dimethyl derivative under elimination of ethane—has never been observed. A qualitative EHMO analysis of conceivable transition states for such a reaction shows that prohibitively high electron repulsion terms arise here from an interaction of the filled e-type molecular orbitals of C_2H_6[37] (involving the carbon p orbitals) with ring and metal electrons at the distance required for a sufficient softening of the C–C bond through electron transfer into the C–C σ^* orbital. For the H_2-insertion reaction, this repulsive interaction is virtually absent due to the absence of filled π-type orbitals and the availability of empty 2p orbitals at about the same energy as that of the σ^* orbital. One might expect then that for molecules with only partly filled e-type orbitals, i.e., for C–C bonds flanked by polarizable π-systems, such as that found in $N{\equiv}CC_6H_5$, this repulsive interaction might be overcome under favorable circumstances by removing much of the π-electron density from the reacting C atoms in the transition state. The corresponding C–C insertion products might be kinetically more easily available in such a case than with other C–C systems.[38] One would further anticipate that C–H bonds would show a behavior intermediate between that of H–H and C–H bonds with respect to accessibility of an insertion reaction transition state. Transition states of this kind are frequently invoked for the reverse of this reaction, i.e., for the reductive elimination of alkanes from alkyl hydride species, a reaction step commonly postulated for catalytic hydrogenation cycles. Intermolecular C–H insertion proper appears to be restricted, however, to cases where the C–H bond is flanked again by a polarizable π-system as in aromatic C–H compounds. The requirements for this type of insertion reaction are to be discussed in the following, final section of this paper.

5. Insertion into Aromatic C–H Bonds. EHMO calculations on conceivable transition states for a concerted[39] C–H insertion require a rather complex parametrization, so that we cannot claim the same degree of validity here as for the reaction with H_2. Nevertheless, several points can clearly be established. As for the stability of the phenyl hydride product, $(C_5H_5)_2WH(C_6H_5)$, a certain degree of ring dislocation appears to be required to minimize repulsion between the ring ligands and the ligated phenyl carbon atom, although both optimal dislocation and energy gained by it are less dramatic here than for the dicarbonyl complex discussed above. Rotation of the phenyl ring about its metal-carbon bond does not lead to significant energy differences between the rotamer with the C_6 ring in the xy plane and that perpendicular to it, but this can obviously only apply to the truncated framework of pseudo-rings employed. When actual C_5H_5 rings are placed into their normal positions, some of their hydrogen atoms would come as close as 1.7 Å to the ortho-hydrogen atom of a C_6H_5 ligand placed perpendicular to the xy plane. Even though some of the ensuing repulsion might obviously be alleviated by geometrical relaxation of the C_5H_5 and/or C_6H_5 ligands, we would expect a sizeable rotational barrier to hold the phenyl rings positioned in the xy plane.

For an analysis of possible transition states in the formation of these phenyl hydride compounds, we limit our discussion to a few obvious geometries (Figure 7, A–D). First, we can rule out a reaction coordinate in which the approach of the benzene substrate to the $(R_5)_2W$ unit would be restricted to the xy plane. For the transition state resulting from such an approach (A), a prohibitively high energy of $+27{,}000\ cm^{-1}$ is predicted in order to place the reacting C–H group in the required proximity to the metal center. In contrast, approach with a benzene molecule perpendicular to the xy plane is found to allow bonding contact of the reacting C–H unit with the metal at an expenditure of about $11{,}000\ cm^{-1}$ if we disregard repulsive interactions between cyclopentadienyl and phenyl hydrogen atoms. Transition state B would therefore appear to be favored over A. There are, however, additional modes of approach for the C_6H_6 molecule to be considered. One such transition state (C) would have the substrate in a configuration similar to that usually postulated for aromatic substitutions, i.e., with a tetrahedral C atom in contact with the metal. For such a structure we find an energy of only $9000\ cm^{-1}$ with respect to the reactants. Our calculations indicate that such a structure can be distorted to that of the final product with little additional expenditure of energy if its C_6 ring is in a rotameric position perpendicular to the xy plane. Finally, we should discuss an additional structure in which one of the C=C bonds of benzene is coordinated to the metal in a fashion similar to that of an olefin complex. Such a species is analogous to the bicyclic intermediates occurring in the reaction of a carbene with aromatic substrates; we calculate a fairly low repulsive energy of about $1000\ cm^{-1}$ for this structure (D). However, the further course of the reaction coordinate from this species to the final product must lead through an unsymmetrically distorted geometry rather sim-

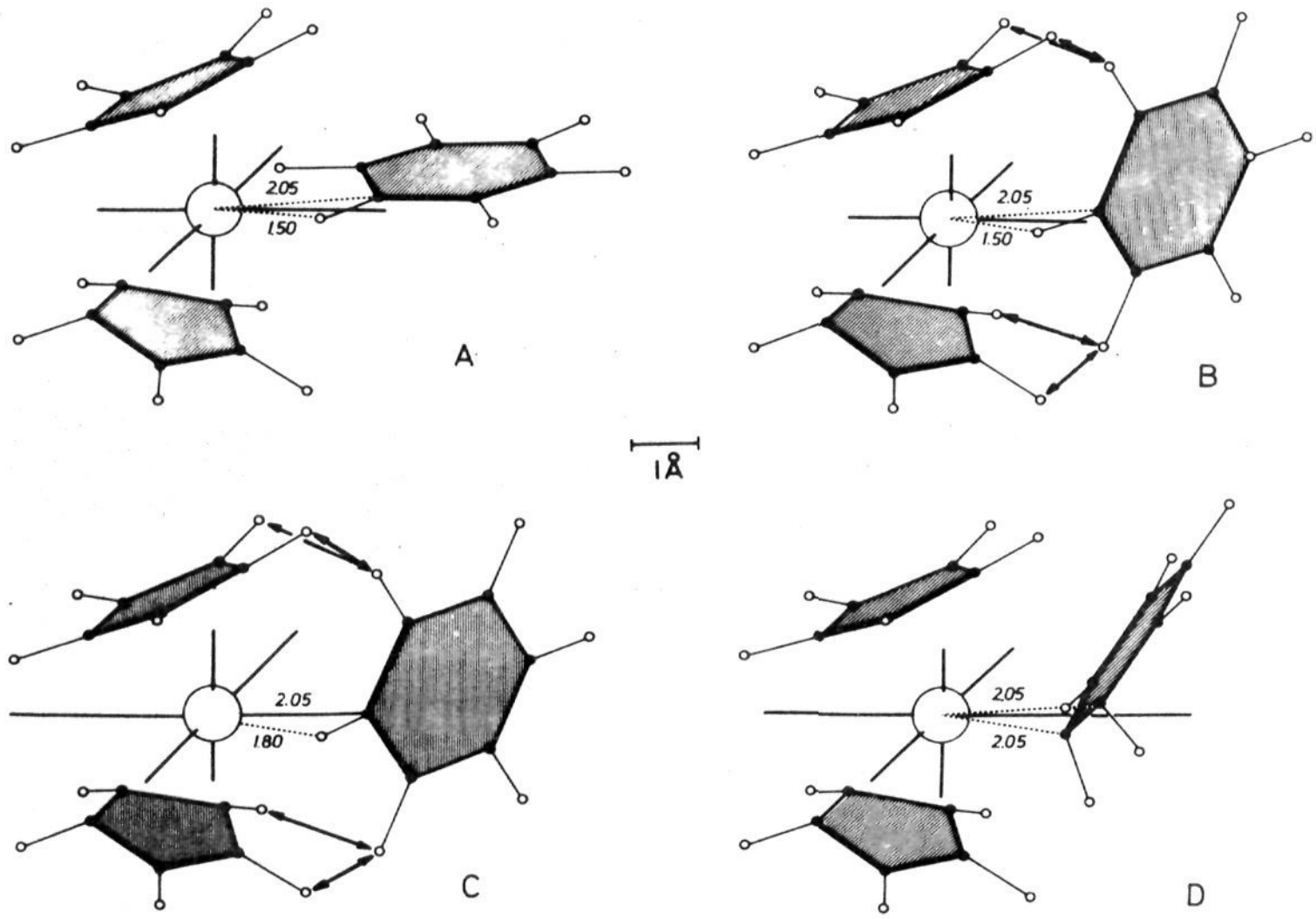

Figure 7. Geometries of conceivable transition states and intermediates for the insertion of $(C_5H_5)_2W$ into a benzene C–H bond.

ilar to that of structure C, so that D could at best be an intermediate on the way to the transition state proper for this reaction. Whether D is in fact associated with an energy minimum along the reaction coordinate, as appears to be the case for carbene reactions, must be left open, since we cannot place sufficient reliance on our computational approach for this complex system.

None the less, our results indicate clearly that in the transition state of the insertion reaction, be it B or C, the reacting carbon atom must be placed into almost-bonding proximity to the metal center, with the C_6 ring remaining perpendicular to the *xy* plane. Such a transition state must therefore have a sizeable repulsive energy contribution, arising from interactions between the C_5H_5 and the ortho-phenyl hydrogen atoms. *To reach such a transition state, it will be an absolute necessity for the metallocene species to accommodate a substantial displacement of its C_5H_5 ligands away from the entering substrate.* We would propose that this requirement is the basis for the reactivity difference observed between the molybdenocene and tungsten intermediates with respect to their capacity for C–H insertion reactions (Table I). The latter appears to accommodate such a ring dislocation with substantially lower energy expenditure, as judged by the critically increased capability of $(C_5H_5)_2W$ to form a stable dicarbonyl complex with a similarly dislocated C_5H_5 ligand geometry.

The relationships discussed above would also provide a natural explanation for the surprising photostability observed for the phenyl hydride complex.[4] In order to reach a nonprohibitive reaction coordinate leading to the photoproducts, the phenyl hydride complex would have to assume a rotameric structure with the phenyl ring perpendicular to the *xy* plane; such a rotamer would not be thermally available, however, as a point of departure for a photodissociation process.

In addition to the one-electron energies discussed so far, the activation energy for a C–H insertion must contain the electron repulsion terms associated with the transition state. In this regard, we can directly transfer the arguments developed above for reactions of H_2 and predict that, e.g., d^2 metallocenes would undergo kinetically more facile insertions than their d^4 counterparts. Even more favorable reaction dynamics would have to be anticipated, however, for a group 5 metallocene hydride intermediate such as $(C_5H_5)_2NbH$. An EHMO analysis of the molecular orbitals of interest predicts for such a species an electron configuration $\Psi_1\Psi_2(^3B_1)$ for both the reactants and the transition state, so that any repulsive contributions would vanish for an insertion reaction of this intermediate. Species of this kind have been invoked as reactive intermediates in kinetically facile and reversible aromatic C–H insertions by Tebbe and Parshall.[40]

Conclusions

In summary, our results would indicate that two contributions not frequently discussed in this context, namely, interelectronic repulsions associated with various metal d-electron configurations and steric encumbrance of coordination sites at the metal center arising from the ring ligands are indeed dominant factors in determining the energy of a transition state for insertion reactions of coordinatively unsaturated metallocene complexes. A satisfactory account for the different complex formation enthalpies of $(C_5H_5)_2Cr(CO)$ and $(C_5H_5)_2Mo(CO)$ is based on the first of these contributions, repulsion among d electrons of the metal center. Similarly, this type of interaction appears to be the leading term for potential energy curves along the reaction coordinate for the formation of dihydrides $(C_5H_5)_2MH_2$. We arrive at the conclusion that the activation energy for an insertion into the H_2 molecule is nearly equal to the spin-pairing energy associated with its transition state.

The unique stability of the dicarbonyl complex $(C_5H_5)_2W(CO)_2$ appears to be associated with a reduced

repulsive interaction between its ligand groups; the same type of facilitated ligand dislocation appears to govern the unique capability of the $(C_5H_5)_2W$ intermediate to undergo sterically demanding insertions into aromatic C-H bonds. This steric encumbrance of coordination sites in coordinatively unsaturated metallocenes, while limitating their reactivity, might be of potential usefulness for the design of catalytic systems with increased selectivity.

NOTE ADDED IN PROOF: J. C. Green, S. E. Jackson, and B. Higginson (*J. Chem. Soc. A*, 403 (1975)) have recently obtained photoelectron spectra for carbonyl, hydride, and other derivatives of molybdenocene and tungstenocene. Our one-electron energies calculated for the highest occupied orbital in these compounds are lower on an absolute scale by about 1.5 eV than the respective values obtained by these authors for vertical ionization. Reasonable agreement exists in terms of relative energy values. The ionization energy for the dihydride Cp_2MoH_2 is reported to be higher by about 0.5 V than that of the carbonyl $Cp_2Mo(CO)$; ionizations from the orbitals a_1 and b_1 (ψ_1 and ψ_2), respectively, which are within less than 1 eV in the carbonyl complex, are separated by 2-3 eV in the dihydride compound; these observations are in accord with the orbital energy correlation diagram given in Figure 1.

References and Notes

(1) (a) Financial support of this work by grants from National Science Foundation (GP 33130X) and Deutsche Forschungsgemeinschaft is gratefully acknowledged. (b) Recipient of a Sloan Fellowship 1973-1974; address correspondence to this author at Universität Konstanz. (c) Recipient of a Barbour Fellowship 1972-1974.
(2) K. L. T. Wong and H. H. Brintzinger, *J. Am. Chem. Soc.*, preceding paper in this issue.
(3) M. L. H. Green and P. J. Knowles, *J. Chem. Soc. A*, 1508 (1971); C. Giannotti and M. L. H. Green, *J. Chem. Soc., Chem. Commun.*, 1114 (1972).
(4) K. L. T. Wong, J. L. Thomas, and H. H. Brintzinger, *J. Am. Chem. Soc.*, **96**, 3694 (1974).
(5) (a) J. L. Thomas and H. H. Brintzinger, *J. Am. Chem. Soc.*, **94**, 1386 (1972); (b) J. L. Thomas, *ibid.*, **95**, 1838 (1973).
(6) L. L. Lohr, Jr. and W. N. Lipscomb, *J. Chem. Phys.*, **38**, 1607 (1963); L. L. Lohr, Jr., and W. N. Lipscomb, *Inorg. Chem.*, **2**, 911 (1963); H. H. Brintzinger and L. S. Bartell, *J. Am. Chem. Soc.*, **92**, 1105 (1970).
(7) M. F. Rettig and R. S. Drago, *J. Am. Chem. Soc.*, **91**, 3432 (1969).
(8) F. A. Cotton and C. B. Harris, *Inorg. Chem.*, **6**, 369, 376, 924 (1967); F. A. Cotton, C. B. Harris, and J. J. Wise, *Inorg. Chem.*, **6**, 909 (1967).
(9) W. C. Herndon and C. H. Hall, *Theor. Chim. Acta*, **7**, 4 (1967).
(10) C. Rappe, *Acta Chem. Scand.*, **20**, 2236 (1966).
(11) A. C. Hopkinson, R. A. McClelland, K. Yates, and I. G. Csizmadia, *Theor. Chim. Acta*, **13**, 65 (1969).
(12) L. C. Allen in "Sigma Molecular Orbital Theory", O. Sinanoglu and K. B. Wiberg, Ed., Yale University Press, Newhaven, Conn., 1970, p 227 f.
(13) R. Hoffmann, *J. Chem. Phys.*, **39**, 1397 (1963).
(14) L. S. Bartell, L. S. Su, and H. K. Yow, *Inorg. Chem.*, **9**, 1903 (1970).
(15) L. L. Lohr, Jr., and W. N. Lipscomb, *Inorg. Chem.*, **3**, 22 (1964).
(16) L. W. Anders, R. S. Hansen, and L. S. Bartell, *J. Chem. Phys.*, **59**, 5277 (1973).
(17) N. A. Beach and H. B. Gray, *J. Am. Chem. Soc.*, **90**, 5713 (1968).
(18) J. D. Dunitz, L. E. Orgel, and A. Rich, *Acta Crystallogr.*, **9**, 374 (1956).
(19) G. P. Gardgrave and D. H. Templeton, *Acta Crystallogr.*, **12**, 28 (1959).
(20) F. Jellinek, *Z. Naturforsch., Teil B*, **14**, 737 (1959).
(21) K. D. Warren, *Inorg. Chem.*, **13**, 1243, 1317 (1974); *J. Phys. Chem.*, **17**, 1681 (1973).
(22) J. S. Griffith, "The Theory of Transition Metal Ions", Cambridge University Press, New York, N.Y., 1961, p 409.
(23) Reference 22, pp 438-439.
(24) Configurations with one or two electrons in π_g are of substantially higher energies and will not be considered for our subsequent analysis of ground state properties. Figures 2 and 3 cannot be used, therefore, to interpret absorption spectra.
(25) M. Gerlock and R. Mason, *J. Chem. Soc.*, 296 (1965).
(26) J. C. Green, M. L. H. Green, and C. K. Prout, *J. Chem. Soc., Chem. Commun.*, 421 (1972).
(27) N. W. Alcock, *J. Chem. Soc. A*, 2001 (1967).
(28) The energy of Ψ_3 (predominantly d_{z^2}) is higher in the carbonyl complex than in the reaction transition state with H_2; one would in fact expect this orbital to interact more strongly with the lone pair of CO than with the σ pair of H_2.
(29) The energy of the alternative singlet state $^1A_1$ arising from $\Psi_1{}^2\Psi_3{}^2$ is also indicated in Figure 6; this state is lower in energy than $^1A_1(\Psi_2{}^2\Psi_1{}^2)$ for small values of α. However, it will not become the ground state anywhere along the reaction coordinate; furthermore, it is so high in energy at the transition state that we have disregarded its interaction with other states in our diagram.
(30) For these calculations, we have included the 2p orbitals of the hydrogen atoms in H_2, since their inclusion was found to lead to a significant decrease of the activation energy as calculated for the transition state discussed above.
(31) J. E. Bercaw, R. H. Marvich, L. G. Bell, and H. H. Brintzinger, *J. Am. Chem. Soc.*, **94**, 1219 (1972).
(32) An excited state of $(R_5)_2MoH_2$ is to be expected about 25,000 cm^{-1} above its ground state from the absorption spectrum of this dihydride. The close vicinity of Ψ_4, Ψ_5, Ψ_2, and Ψ_3 for this compound precludes an assignment of this lowest excited state.
(33) From Table V, we derive electron repulsion energies of $3A - 12B$ for the reactant quartet ground state $^4B_1(\Psi_1\Psi_2\Psi_3)$ and of $3A + 4B(3 - 2\alpha^2)/(1 + \alpha^2) + 4C$ or roughly $3A + 2B + 4C$ for the $^2A_1$ term at the transition state state ($\alpha \approx 1$) of the insertion reaction. The spin-pairing energy at the transition state, and hence the approximate activation energy would thus amount to about $14B + 4C$ for a d^3 system, as compared to about $12B + 3C$ for an analogous d^4 reaction system.
(34) For a d^2 metallocene, the probable reactant ground state $^3B_1(\Psi_2\Psi_3)$ has an electron repulsion energy of $A - 8B$; for the transition state configuration $\Psi_1\Psi_2$ (also $^3B_1$) one obtains $A + 4B(1 - 2\alpha^2)/(1 + \alpha^2)$ (Table V) or roughly $A - 2B$, for $\alpha \approx 1$. The electron repulsion contribution to the activation energy is now reduced to about $6B$ or less, because of an interaction term connecting the two $^3B_1$ states.
(35) For an electron configuration with less than two d electrons, Figure 1 indicates a decreased binding energy in the product, due to an insufficient utilization of the low-lying component of Ψ_2; in chemical terms, at least two d electrons are needed, of course, for an oxidative addition reaction.
(36) J. E. Bercaw, *J. Am. Chem. Soc.*, **96**, 5087 (1974). The reverse reaction, the reductive elimination of H_2, is fast initially but complicated by the fact that the titanocene thus generated will react with residual dihydride to form a Ti(III) hydride species which loses H_2 only slowly.
(37) See, for example, W. L. Jorgenson and L. Salem, "The Organic Chemist's Book of Orbitals", Academic Press, New York, N.Y., 1973.
(38) Oxidative addition of C_6H_5CN to $Pt(P(C_2H_5)_3)_3$ under C-C bond cleavage has been reported by D. H. Gerlach, A. R. Kane, G. W. Parshall, J. P. Jesson, and E. L. Muetterties, *J. Am. Chem. Soc.*, **93**, 3543 (1971).
(39) The concerted nature of this insertion reaction is supported by competition experiments with isotopically labeled substrates; K. L. T. Wong and H. H. Brintzinger, unpublished results
(40) F. N. Tebbe and G. W. Parshall, *J. Am. Chem. Soc.*, **93**, 3793 (1971).